A Study on Fatigue Crack Propagation Mechanism of GFRP in Synthetic Sea Water

Yon Jig Kim, Jae Kyoo Lim*

Faculty of Mechanical Engineering, Automobile Hi-Technology Research Institute, Chonbuk National University, Chonju 561-756, Korea

This paper evaluates the fatigue fracture behavior of a chopped strand glass mat/polyester composite both in air and sea water. Bending fatigue(R=-1) was performed on dry and wet specimens, that is respectively in air and sea water. Where the pH concentration of sea water was controlled to 6. 0, 8. 2, 10. 0 and the wet specimens were immersed in the sea waters for 4 months. Throughout the tests, fatigue cracks both in the dry and wet specimens, tested in the air or sea water, occurred at the beginning of the cycle, followed by either of two regions : one decreasing and the other increasing as the crack growth rate increases.

Key Words : Glass Fiber Reinforced Plastic, Fiber-Matrix Debonding, Hand Lay Up, Fiber Pull-Out, Crack Bridging, Fatigue Crack Propagation Mechanism, pH Concentration,

1. Introduction

Just as in the case of static failure, fatigue failure mechanisms in fiber reinforced composites are quite different from those in monolithic, homogeneous materials such as metals. Fatigue failure in metals, for example, occurs as a result of initiation and growth of a principal crack. Fiber reinforced laminate composites, on the other hand, can sustain a variety of subcritical damages, such as matrix fracture, fiber-matrix debonding, fiber pull-out and fiber crack bridging(Price, 1989 ; Hahn and Lorenzo, 1984). Fatigue crack propagation mechanism mentioned depends on the type of composites, the function of the structure and relevant conditions such as stress and environment. Under many circumstances, composites are superior to metals in their fatigue resistance. However, our present knowledge of the fatigue and fatigue damage in composites is incomplete and more researchs should be required.

Failure of Glass Fiber Reinforced Plastics (GFRP) in ocean structures such as floating structures, harbor facilities, yachts and minesweepers occurs due to the combined action of service load and sea water, but the study of their fracture behavior in sea water is unusual (Kim and Lim, 1997). Therefore, the purpose of this study is to describe a mode of fatigue crack growth behavior of GFRP in air and sea water. We examine laminates made from chopped strand mat type E-glass, which is used as a common resin and also polyester resin which has been used for many years in applications requiring resistance to chemical attack.

* Corresponding Author,
E-mail:yonjig@intizen.com/jklim@moak.chonbuk.ac.kr
TEL : +82-63-270-2321; **FAX** : +82-63-270-2460
Faculty of Mechanical Engineering, Automobile Hi-Technology Reserch Institute, Chonbuk National University, Chonju 561-756, Korea. (Manuscript **Received** November 30, 2000; **Revised** July 24, 2001)

2. Experimental Procedure

2.1 Materials

GFRP plates fabricated according to Hand Lay Up (HLU) (Milewski and Katz, 1987) are used throughout this investigation. Polyester resin, the matrix material of GFRP, is vinylester type epoxy acrylate resin and chopped strand mat (CSM) E-glass fiber is used as the reinforcement. The

Table 1 Chemical composition and mechanical properties of E-glass fiber

(a) Composition (wt.%)

SiO_2	Al_2O_3	B_2O_3	CaO, MgO	Na_2O	K_2O	Fe_2O_3	F_2
55.2	14.8	7.3	22.0	0.3	0.2	0.3	0.3

(b) Mechanical properties (25℃)

Filament tensile strength (MPa)	Coefficient of thermal expansion (10^{-6}/℃)	Young's modulus (MPa)
3,626	5.0	75,460

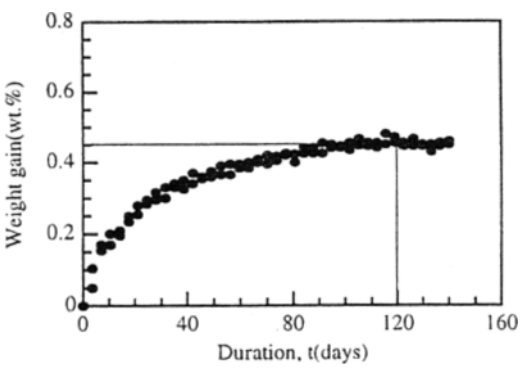

Fig. 1 Diffusion behavior of synthetic sea water into GFRP at room temperature

filaments are surface-treated with an epoxy-compatible silane finish by the manufacturer.

During preparing GFRP plates, one surface mat (SM) is, first, placed on the ground, four CSM, in turn, laid up and finally one SM put on the upper surface. This plate is subjected to room temperature for 24 hours followed by a post cure 2 hours at 120℃. The plate has a final thickness of 3.2 mm and a fiber content of 30 ~ 35 (wt.%). The chemical properties of E-glass fiber are shown in Table 1.

2.2 Sea water absorption

A synthetic sea water recommended by ASTM D 1141 (ASTM, 1975) is used in this test with pH concentration of 6.0, 8.2, 10.0.

The specimens for test of sea water absorption are machined in the form of a bar 76.2 mm long by 25.4mm wide by the thickness of the sheet as made above (3.2mm). These specimens are soaked in each synthetic sea water at room temperature and weighed at various time intervals to determine the rate of sea water absorption. The sea water absorption rate does not change according to pH concentration of synthetic sea water and saturated at 0.45wt. % as shown in Fig. 1. A more detailed description of the test procedure is referred to by ASTM D 570 (ASTM, 1981).

Table 2 Designated specimens in specific condition

Environment / Specimen	Synthetic sea water			Air
	pH6.0	pH8.2	pH10.0	
Dry specimen	AS60	AS82	AS10	AA
Wet specimen	SS60	SS82	SS10	-

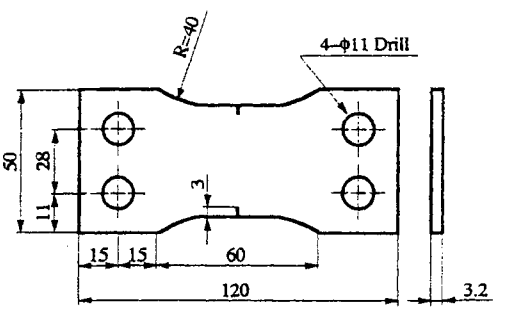

Fig. 2 Dimension of specimen for fatigue test

2.3 Specimens

The resulting plates are finally machined into specimens indicated in Fig. 2 by JIS K 7119 (JIS, 1972). In this test, two types of specimens are used : a dry specimen cured for 2 hours at 50±3℃ before testing, and a wet specimen immersed to be saturated in synthetic sea water for 4 months. The sea water absorption rate of the wet specimen is 0.45%.

In this test, we shall designate specimens as in Table 2 for the test conditions of GFRP.

2.4 Test method

A double-edge notched specimen is used in the bending fatigue test and three specimens are tested in each conditions. Fatigue testing is performed on a Repeated Torsion & Bending Fatigue Testing Machine programmed to cycle sinusoidally in R = −1 at 30Hz.

Crack length is measured using a traveling microscope positioned in front of the specimen.

Environmental testing is done using a synthetic sea water and a lucite-walled chamber is installed around the testing apparatus for measurements on the immersed specimens. Fracture surface is evaluated using both an optical and a scanning electron microscope (SEM).

2.5 Data analysis

Upon crack initiation at machined notch, the testing machine is stopped at even time intervals to record the crack length, a, and the corresponding number of cycles, N. The values of a are then plotted versus N and a best-fit curve is drawn. From such a graph, the crack growth rate, da/dN, is obtained by measuring the slope of the curve at various values of a.

In this paper, we use the stress intensity factor, K, recommended by The Japanese Society of Materials Science is expressed as (JSMS, 1980),

$$K=f\left(\frac{a}{w}\right)\cdot\sigma_b\sqrt{\pi a}$$

$$f\left(\frac{a}{w}\right)=1.98+0.36\left(\frac{a}{w}\right)-2.12\left(\frac{a}{w}\right)^2+3.42\left(\frac{a}{w}\right)^3$$

where σ_b is applied bending stress and $f(a/w)$ is a parameter depending on the specimen and crack geometries. For R=−1, the K_{min} is zero because the fatigue crack is closed. Therefore, note in this paper that the stress intensity factor range (ΔK) is $\Delta K=K_{max}$.

3. Test Results and Discussion

3.1 Fatigue life

The S-N curves obtained under air and synthetic sea water with dry and wet specimens are shown in Fig. 3.

The fatigue limit is not observed in range up to 10^7 cycles. This is the common feature of GFRP (Dharan, 1975). Moreover, the fatigue lives of AS and SS materials are considerably less than that of AA and the fatigue life of GFRP in synthetic sea water decreases with the pH concentration increase. This behavior is due to the hardening of resin in synthetic sea water as pH concentration increases (Fig. 4) and, in addition, it has been reported that the glass fibers are rapidly corroded

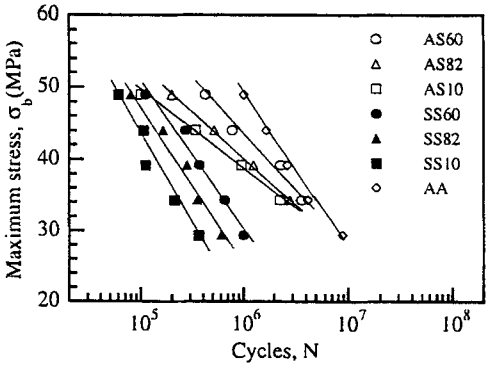

Fig. 3 S-N curves of dry and wet specimens tested in air or synthetic sea water

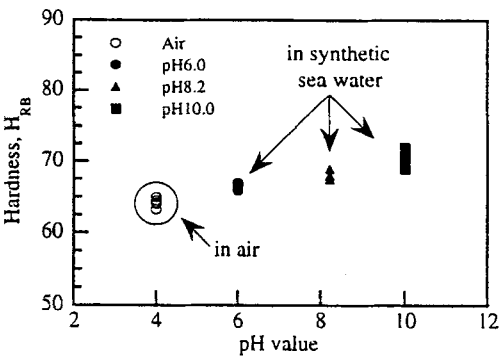

Fig. 4 Relation between hardness of resin and pH value in synthetic sea water(980N)

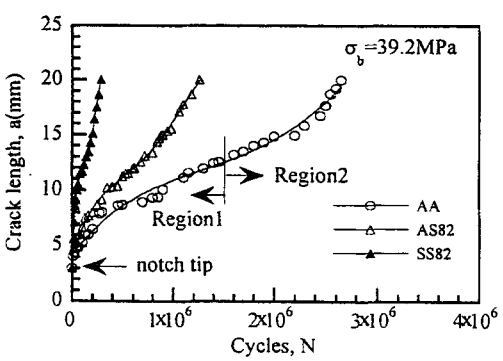

Fig. 5 Crack length versus number of cyctes.

when the concentration of OH^- ranges from pH9.5 to pH10.0 (Schmitz and Metcalfe, 1966; Ishai, 1975).

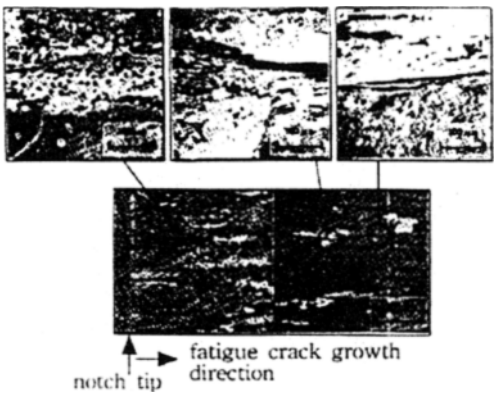

Photo 1 Axial cracking along the fiber-matrix interface in the load direction of dry specimen tested in air(AA)

3.2 Fatigue crack propagation behavior

Three typical a-N curves of AA, AS82 and SS82 obtained under a repeated bending fatigue test (R=−1) are shown in Fig. 5.

It is difficult to observe the crack acceleration area before stable crack propagation, as generally occurs for metals because fatigue crack is occurred at the beginning of the cycle and rapidly propagates. Accordingly, if we look at the whole fatigue crack propagation behavior, the curves can be divided into two regions : Region 1 indicates crack deceleration and Region 2 represents crack reacceleration. It has been known that these regions occur under a compressive fatigue process (Kunz and Beaumont, 1975).

Photo 1 illustrates an SEM fractograph of AA material tested in air. This fractograph confirmed an axial cracking through the fracture surface. It is found that debonding and delamination is more developed than splitting.

Consequently, the fatigue crack growth can be explained in the following way. The crack that has been initiated at the beginning of this test grows rapidly under the applied stress and then visibly slows down because of the axial cracks such as debonding and delamination which reduce the magnitude of the stress field at the crack tip and cause deceleration of the advancing crack. Subsequent axial cracking get to the limit and this reaccelerates the fatigue crack growth because the ligament of the specimen is reduced, and then the unstable crack growth occurs.

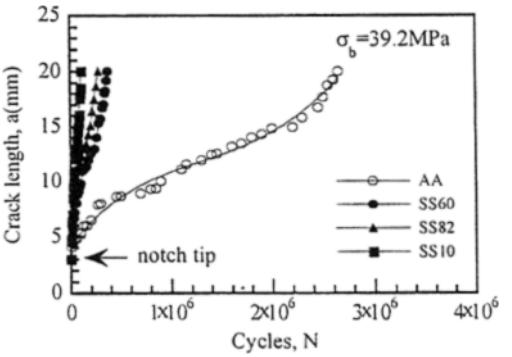

Fig. 6 Crack length versus number of cycles

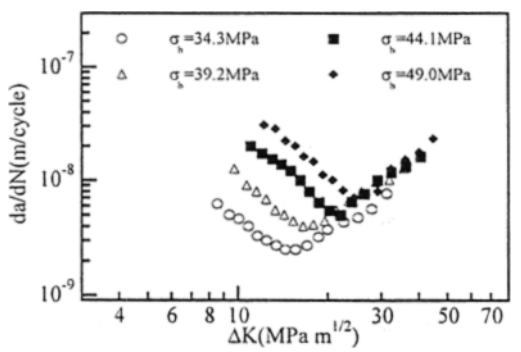

Fig. 7 Relation between crack growth rate and stress intensity factor range of the dry specimen tested in air

From Fig. 5 it can be seen that the fatigue crack growth mode of GFRP in synthetic sea water is not different from the mode in air and the process of AS82, SS82 is faster than that of AA. Therefore, it should be moted that the synthetic sea water promotes rapid progress in the fatigue crack growth.

Figure 6 shows the a-N curves according to the pH concentration of synthetic sea water for wet specimens. In this figure, it appears that the crack propagation is fast as the pH concentration increase. This behavior is due to the hardening of the resin (Fig. 4) and is caused by degradation of the interfacial strength between fiber and resin as pH concentration increases (Kim and Lim, 1992 ; Kim and Lim, 1997).

Crack growth rate (da/dN) as a function of ΔK can be obtained at consecutive positions

along a-N curves. A typical log-log plot of da/dN versus ΔK for AA materials is shown schematically in Fig. 7.

These curves have a V-shape that can be divided into two major regions and confirm the existence of a transition point where the fatigue crack growth changes from deceleration to acceleration. In this figure, we think that the point depends on the load because the point shift to large ΔK value as the applied stress increase. On the other hand, the point is independent of the environmental condition because the points of SS materials are located in the same ΔK values as AA materials as shown in Fig. 8.

Figure 9 shows the relation between da/dN and ΔK for SS materials as σ_b=39.2MPa. It can be seen that the fatigue crack growth rate in alkaline sea water is very high because the rate of SS10 is higher than that of any other specimens and the transition point is independent of pH concentration in sea water.

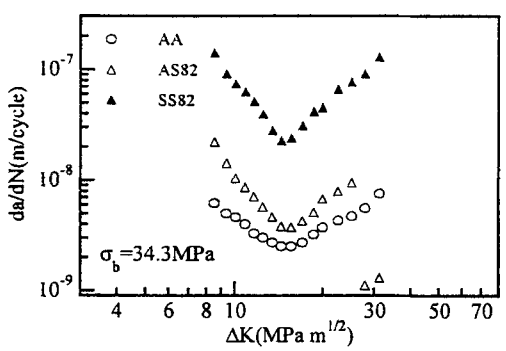

Fig. 8 Relation between crack growth rate and stress intensity factor range.

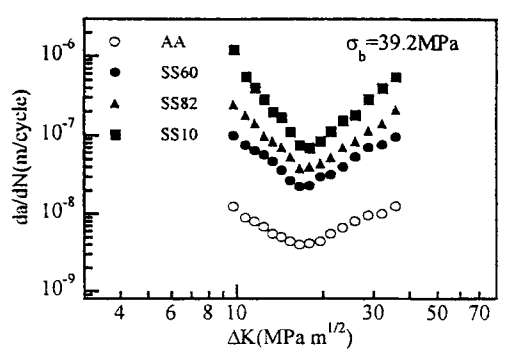

Fig. 9 Relation between crack growth rate and stress intensity factor range

3.3 Fatigue crack propagation mechanism

In general, the fatigue crack propagation behavior for conventional materials can be divided into three regions (Knott, 1979). The behavior in region I exhibits a fatigue-threshold cyclic stress intensity factor range, ΔK_{th}, below which cracks do not propagate under cyclic stress. Region 2 represents the stable crack propagation behavior and in region 3 the fatigue crack growth rate is higher than that predicted for region 2. However, in this study we can observe something remarkable about the crack propagation behavior, that is, the behavior can be divided into two regions and confirms the existence of transition point. From these experimental observations we can discribe the fatigue crack propagation process as shown in Fig. 10.

In this figure, (a) is a schematic diagram in cross section of the specimen and describes its state before test. The hatched portion on the left side of the cross section is a prenotch in depth of 3 mm and the right side is a central position of the specimen. At the beginning of test, the fatigue crack initiates and propagates from the notch tip and the crack proceedes with a visible increase in velocity because the axial cracks, attributed to elastic buckling of fibers, are very small and few

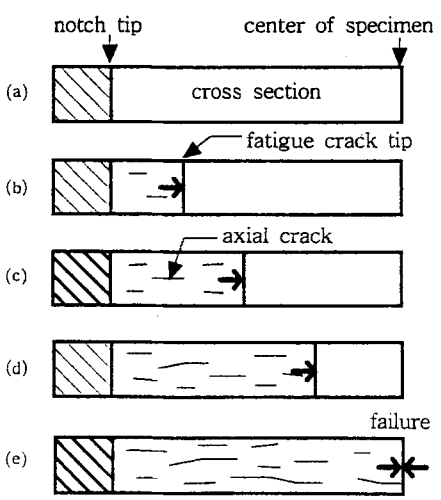

Fig. 10 The situation of fatigue crack growth and the model for axial cracking

as shown in (b). Continued cycling produces many cracks in the axial direction is perpendicular to the cross section as shown in (c) and these cracks constrained the fatigue crack propagation. After a number of cycles, the axial cracking get to the limit and this reaccelerate the fatigue crack growth because the ligament of the specimen is reduced as shown in (d), and then complete failure resulted from the unstable fatigue crack growth as shown in (e).

4. Conclusions

Through this test, we ascertained a particular mode of fatigue crack propagation for CSM type E-glass fiber reinforced polyester resin composite tested in air and synthetic sea water. The fatigue crack propagation behavior is composed of deceleration and acceleration processes. The transition point of fatigue crack propagation depends on the load, while the point is independent of the environmental condition. But as its pH concentration increases the sea water promotes axial cracks such as debonding and delamination and further decelerate and accelerate cracking. Moreover, it is found that the fatigue life of GFRP in synthetic sea water is considerably less than its life in air and is decreased with increase in pH concentration. This behavior is due to the hardening of the resin and is caused by reduction of interfacial strength between fiber and resin as pH concentration increases.

References

ASTM D 1141, 1975, "Standard Specification for Substitute Ocean Water."

ASTM D 570, 1981, "Standard Test Method for Water Absorption of Plastics."

Dharan, C. K. H., 1975, "Fatigue Failure Mechanisms in a Unidirectionally Reinforced Composite Material," *Fatigue of Composite Material, ASTM STP 569*, pp. 171~188.

Hahn, H. T. and Lorenzo, L., 1984, *in Advances in Fracture Research*, ICF6, New Delhi, India, Pergamon Press, Oxford, Vol. 1, p. 549.

Ishai, O., 1975, "Environmental Effects on Deformation, Strength and Degradation of Unidirectional Glass-Fiber Reinforced Plastics," *Polym. Eng. Sci.*, Vol. 15, No. 7, pp. 486~490.

JIS K 7119, 1972, "Testing Method of Flexural Fatigue of Rigid Plastics by Plane Bending."

Kim, Y. J. and Lim, J. K., 1992, "Synthetic Sea Water and Strain Rate Effects on Tensile Properties of E-Glass/Polyester Composites," *Korean Journal of Materials Research*, Vol. 2, No. 2, pp. 133~142.

Kim, Y. J. and Lim, J. K., 1997, "A Study on Properties of Corrosion Fracture Surfaces of GFRP in Synthetic Sea Water," *KSME International Journal*, Vol. 11, No. 3, pp. 249~254.

Knott, J. F., 1979, Fundamentals of Fracture Mechanics, Tower Press, pp. 246~251.

Kunz, S. C. and Beaumont, P. W. R., 1975, "Microcrack Growth in Graphite Fiber-Epoxy Resin Systems During Compressive Fatigue," *Fatigue of Composite Materials, ASTM STP 569*, pp. 71~91.

Milewski, J. V. and Katz, H. S., 1987, "Handbook of Reinforcements for Plastics," Van Nostrand Reinhold, New York, pp. 267~275.

Price, J. N., 1989, "Stress Corrosion Cracking in Glass Reinforced Composites," *Fractograph and Failure Mechanisms of Polymers and Composites*, Elsevier Applied Science, London and New York, pp. 495~531.

Schmitz, G. K. and Metcalfe, A. G., 1966, "Stress Corrosion of E-glass Fibers," *Ind. Eng. Chem.*, Res & Dev., Vol. 5, No. 1, pp. 1~8.

The Japanese Society of Materials Science, 1980, "Data Book of Resistance of Fatigue Crack Propagation," *The Japanese Society of Materials Science*, p. 32.